Severe acute respiratory syndrome coronavirus 2 (SARS-CoV-2) infections by intranasal or testicular inoculation induces testicular damage preventable by vaccination in golden Syrian hamsters

Can Li[1,2†], Zhanhong Ye[1†], Anna Jin-Xia Zhang[1,2,3†], Jasper Fuk-Woo Chan[1,2,3,4,5,6†], Wenchen Song[1,2], Feifei Liu[1], Yanxia Chen[1], Mike Yat-Wah Kwan[7], Andrew Chak-Yiu Lee[1,2], Yan Zhao[1], Bosco Ho-Yin Wong[1,2], Cyril Chik-Yan Yip[4], Jian-Piao Cai[1], David Christopher Lung[8], Siddharth Sridhar[1,2,3,4], Dongyan Jin[6,9], Hin Chu[1,2,3], Kelvin Kai-Wang To[1,2,3,4], Kwok-Yung Yuen[1,2,3,4,5,6*]

[1]State Key Laboratory of Emerging Infectious Diseases, Carol Yu Centre for Infection, Department of Microbiology, Li Ka Shing Faculty of Medicine, The University of Hong Kong, Pokfulam, Hong Kong Special Administrative Region, China

[2]Centre for Virology, Vaccinology and Therapeutics, Hong Kong Science and Technology Park, Hong Kong Special Administrative Region, China

[3]Department of Clinical Microbiology and Infection Control, The University of Hong Kong-Shenzhen Hospital, Shenzhen, China

[4]Department of Microbiology, Queen Mary Hospital, Pokfulam, Hong Kong Special Administrative Region, China

[5]Academician Workstation of Hainan Province, and Hainan Medical University-The University of Hong Kong Joint Laboratory of Tropical Infectious Diseases, Hainan Medical University, Haikou, China; and The University of Hong Kong, Pokfulam, Hong Kong Special Administrative Region, China

[6]Guangzhou Laboratory, Guangdong Province, China.

[7]Department of Paediatrics, Princess Margaret Hospital, Hong Kong Special Administrative Region, China

[8]Department of Pathology, Queen Elizabeth Hospital / Hong Kong Children's Hospital, Hong Kong Special Administrative Region, China

[9]School of Biomedical Sciences, The University of Hong Kong. Hong Kong Special Administrative Region, China

[†]These authors are co-first authors.

***Correspondence:** K.-Y. Yuen, State Key Laboratory of Emerging Infectious Diseases, Carol Yu Centre for Infection, Department of Microbiology, Li Ka Shing Faculty of Medicine, The University of Hong Kong, Pokfulam, Hong Kong Special Administrative Region, China; and Department of Clinical Microbiology and Infection Control, The University of Hong Kong-Shenzhen Hospital, Shenzhen, China (kyyuen@hku.hk)

Summary: SARS-CoV-2 intranasal infection causes testicular damage and associated hormonal changes despite a self-limiting pneumonia in hamsters. Awareness of possible hypogonadism and subfertility is important in managing convalescent COVID-19 males.

ABSTRACT

Background. The role of SARS-CoV-2 in the pathogenesis of testicular damage is uncertain.

Methods. We investigated the virological, pathological, and immunological changes in testes of hamsters challenged by SARS-CoV-2 wild-type and its variants by intranasal or direct testicular inoculation using influenza virus A(H1N1)pdm09 as control.

Results. Besides self-limiting respiratory tract infection, intranasal SARS-CoV-2 challenge caused acute decrease in sperm count, and serum testosterone and inhibin B at 4 to 7 days post-infection (dpi), and subsequently reduced testicular size and weight, and serum sex hormone level at 42 to 120 dpi. Acute histopathological damage with varying degree of testicular inflammation, haemorrhage, and necrosis, degeneration of seminiferous tubules and disruption of orderly spermatogenesis were seen with increasing virus inoculum. Degeneration and necrosis of Sertoli and Leydig cells were found. Though viral loads and SARS-CoV-2 nucleocapid (N) protein expression were markedly lower in testicular than lung tissues, direct intra-testicular injection showed N expressing interstitial cells and epididymal epithelial cells. Control intranasal or intra-testicular challenge by A(H1N1)pdm09 showed no testicular infection or damage. From 7 to 120 dpi, degeneration and apoptosis of seminiferous tubules, immune complex deposition and depletion of spermatogenic cell and spermatozoa persisted. Intranasal challenge with Omicron and Delta variants could also induce similar testicular changes. These testicular damages can be prevented by vaccination.

Conclusions. SARS-CoV-2 can cause acute testicular damage with subsequent chronic asymmetric testicular atrophy and associated hormonal changes despite a self-limiting pneumonia in hamsters. Awareness of possible hypogonadism and subfertility is important in managing convalescent COVID-19 males.

Keywords: hamster; coronavirus; COVID-19; SARS-CoV-2; testicle

INTRODUCTION

Severe acute respiratory syndrome coronavirus 2 (SARS-CoV-2) has caused the devastating Coronavirus Disease 2019 (COVID-19) pandemic[1]. Though COVID-19 is primarily a respiratory infection, involvements of many extrapulmonary tissues from olfactory sensory system to reproductive tract have been reported[2, 3]. COVID-19 associated testicular pain was reported to be more frequent than expected[4, 5]. In a human challenge study, one in 18 SARS-CoV-2 infected volunteer developed epididymal discomfort[6]. One postmortem study of COVID-19-infected males revealed orchitis with extensive germ cell and Leydig cell destruction[7]. Semen specimens of four acute and two recovered COVID-19 cases were SARS-CoV-2 positive by RT-PCR though this was not consistently found in recovered patients[8, 9]. Whether SARS-CoV-2 can cause testicular damage in COVID-19 is still uncertain. We investigated the temporal profiles of virological, pathological, immunological, and hormonal changes of hamsters challenged by intranasal or direct testicular administration of wild-type and variant SARS-CoV-2 with A(H1N1)pdm09 influenza virus as a control.

METHODS

Animal, Virus and Biosafety

Eight-ten weeks old male Syrian hamsters were infected with SARS-CoV-2 wild-type strain HK-13 (GenBank accession number: MT835140), and Delta (GISAID:EPI-ISL-3221329) and Omicron (GISAID:EPI-ISL-7138045) variants[10]. A(H1N1)pdm09 (A/HK/415742/2009) influenza mouse-adapted strain was used as control [11]. Experiments involving live SARS-CoV-2 followed the approved standard operating procedures of the Biosafety Level (BSL)-3 facility [12, 13]. Experimental details are included in supplementary methods.

Intranasal Virus inoculation and vaccination

Hamsters were intranasally challenged with 10 to 10^5 plaque forming units (PFU) of SARS-CoV-2 strains or A(H1N1)pdm09 10^3 or 10^5 PFU in 50 µl volume under anesthesia [12]. The animals were sacrificed for analysis at 1 day-post-infection (dpi), 4dpi, 7dpi, 42dpi or 120dpi together with mock infection controls. Formalin inactivated SARS-CoV-2 HK-13 whole virion vaccine (10ug of total protein per hamster) was given in testicular protection experiment using PBS as control [14].

Intratesticular virus inoculation

SARS-CoV-2 HK-13 or A(H1N1)pdm09 at 10^5PFU in 50µl were injected transcutaneously into the testis using a 27G needle under anesthesia. The mock controls were injected with 50µl of PBS. The animals were sacrificed at 1dpi or 4dpi.

Testis weight and sperm count

At the time of sampling, testes were dissected from the epididymis and weighed. Freshly excised epididymis was incised in 1mL PBS. Sperms were collected after 15min and counted in a hemocytometer.

Viral load assays, histopathological examination and cytokine and chemokine profiling

Testicular viral loads, histopathology, immunohistochemistry, apoptosis marker, and cytokine/chemokine profiles, were performed as we described previously[11, 12, 15]. Detailed protocols were provided in supplementary methods. Specific primers and probes for SARS-CoV-2 RNA-dependent-RNA-polymerase gene, influenza Matrix gene(M), and cytokine/chemokine for real-time PCR assay were listed Table S1.

Paraffin sections of testes were stained by Hematoxylin and eosin(H&E). Biomarkers for seminiferous tubular germ cells and Sertoli cells were stained by immunohistochemical method with antibodies to “deleted in azoospermia like” protein (DAZL) and vimentin, respectively.

SARS-CoV-2 nucleocapsid protein (N) or influenza viral nucleoprotein(NP) expression in testes were stained with a rabbit antibody against SARS-CoV-2 N protein [12] or mouse anti-influenza NP antibody[11][16]. Histological examination was conducted in a blinded manner. The damages in testicular tissue were scored using Johnsen's Score criteria with minor modification(Table S2)[17, 18]. Apoptosis was detected by Click-iT® Plus TUNEL assay kit and scored semi-quantitatively [10].

Enzyme immunoassay (EIA) for male sex hormone

Morning serum total testosterone and inhibin B were detected by hamster EIA Kits (MyBioSource, CA).

Statistical Analysis

Statistical analyses for significant differences(p<0.05) were performed with Student's t-test or Fisher's exact test to compare between infection and mock control groups (GraphPad Prism8).

RESULTS

Acute testicular damage upon intranasal challenge of hamsters with SARS-CoV-2

Male hamsters were intranasally inoculated with 10, 10^2, 10^3 or 10^5PFU of wild-type SARS-CoV-2(Figure 1A). Self-limiting histological changes of pneumonia were similar to what we previously reported [12]. No scrotal swelling was clinically detectable in any animal at any time point. Sperm counts were significantly reduced in all hamsters at 4dpi after 10^3 or 10^5PFU infection (Figure 1B), despite absence of gross pathological changes in appearance, size or weight (Figure 1C-D). Serum testosterone and inhibin B levels were significantly lower at 4dpi and 7dpi comparing to the mock control (Figure 1E). The findings are consistent with subclinical testicular damage during the acute phase of SARS-CoV-2 infection.

Chronic testicular damage after intranasal challenge by SARS-CoV-2

Significantly reduced size and weight of testes at 120dpi was observed (Figure 2A&B). Sperm counts were significantly reduced at 42 and 120dpi (Figure 2C). Serum testosterone and inhibin B levels were significantly reduced at 120dpi (Figure 2D). Table 1 summarizes findings at different time points after 10^3PFU infection which indicates that testicular and hormonal changes occurred long after the lungs have recovered from SARS-CoV-2 infection.

Histopathological changes of acute testicular damage in SARS-CoV-2 infection

The normal structure of mock-control testis showed seminiferous tubules consisting of multilayers of germline epithelial cells neatly arranged with mature spermatozoa in the lumen (Figure 3A). At 1dpi after 10^5PFU intranasal challenge, 33%(2/6) hamsters had expanded testicular interstitial space due to edema. Though the multilayer structure remained intact, mild segmental seminiferous epithelial degeneration and germ cell sloughing were observed (Figure S1). At 4dpi, severe testicular hemorrhage and interstitial mononuclear cell infiltration were observed in 18.7%(3/16) of hamsters (Figure 3B). Severe seminiferous tubular necrosis with occasional neutrophils, and disordered germ cells arrangement with reduced layers of spermatogenic cell spectrum were found in 43.8% (7/16) of hamsters. Multinucleated germ cell degeneration and even depletion of luminal spermatozoa was frequently observed (Figure 3C). 47.06%(8/17) of the hamsters infected with 10^3PFU showed testicular damages at 4dpi which generally had less severe and more patchy than the 10^5PFU group.

At 7dpi, severe testicular necrosis in both 10^3 and 10^5PFU infected hamsters were observed. Some seminiferous tubular lumens only contained cell debris(Figure 3D). Significantly lower Johnsen's scores at 4 and 7dpi after SARS-CoV-2 infection(Figure 3E, table 1) indicated

substantial impairment of spermatogenesis. The epididymis had interstitial mononuclear cell infiltration with lumens filled with sloughed germ cells and cell debris (Figure 3F). No detectable histopathological changes were observed at 4dpi after challenge with10PFU or 10^2PFU (Figure S1).

Degeneration and necrosis of Sertoli cells and spermatogenic cells after intranasal SARS-CoV-2 infection

Sertoli cells with long cytoplasmic arms extending towards the lumen situated at the basal membrane of the seminiferous tubules are supportive cells that nourish and support orderly germ cell differentiation. Sertoli cells expressing high levels of cytoplasmic vimentin were regularly distributed as radiant pattern from the basal membrane towards the lumen (Figure 4A). Severely disrupted distribution pattern of vimentin expressing Sertoli cells was seen at 4dpi after 10^5PFU infection (Figure 4B). Cytoplasmic vacuolation, degeneration and detachment of Sertoli cells into the lumen were also found (Figure 4B).

The DAZL protein was generally more readily expressed in primary spermatocytes than spermatogonia but not in secondary spermatocytes and Sertoli cells (Figure 4C). In intranasal 10^5PFU challenged hamsters at 4dpi, DAZL staining demonstrated disarray of germ cell arrangement, and DAZL positive multinucleated giant cells formed from primary spermatocytes, together with many DAZL negative sloughed germ cells and multi-nucleated giant cells formed from secondary spermatocytes (Figure 4D). Affected primary spermatocytes and secondary spermatocytes were accompanied by ballooning changes of adjacent Sertoli cells. Interstitial Leydig cells showed nuclear condensation indicative of apoptosis (Figure 4E).

Testicular infection by intranasal or direct intratesticular injection with SARS-CoV-2

Unlike highly infected lung tissues, low viral loads were found in only a few testicular samples at 4, 7, 42 and 120dpi (Figure 5A). Immunofluorescent staining of viral N protein showed only a few positive cells in seminiferous tubules and detached cells in epididymal lumen at 4dpi (Figure 5B). Sperm smear also showed a few N positive sloughed cells (Figure 5C).

Direct intratesticular injection induced localized interstitial inflammatory infiltration and segmental seminiferous tubular degeneration 4dpi (Figure 5D). But N-protein was readily seen in the interstitium and epididymis epithelial cells as multiple foci with each containing 3-5 immunofluorescence positive cells at 1dpi and 4dpi (Figure 5D&E). As 5 out of 6 testes had detectable viral loads while 2 had subgenomic RNA (sgRNA) expression, SARS-CoV-2 has likely replicated in testicular cells (Figure 5F). Significantly increased cytokine/chemokine mRNA in testes were detected after intratesticular injection of SARS-CoV-2 at 1dpi and 4dpi (Figure 5G). In contrast to SARS-CoV-2-injected hamsters, influenza viral antigen was rarely found in testes after A(H1N1)pdm09 injection and no histopathological changes were observed despite marginally detectable viral load and increased mRNA expression for cytokine/chemokine (FigureS2). Together, our results reveal that testicular cells can be infected when exposed to SARS-CoV-2 which triggers cytokine/chemokine responses and cell damage.

Inflammatory cytokine/chemokine mRNA expression profiles and apoptosis regulatory genes in testes of hamsters challenged intranasally.

Because only some hamsters developed testicular damage (Table 1), only their testicular cytokine/chemokine levels were compared with mock-controls. Proinflammatory cytokine/chemokine including IFN-α, IFN-γ, IL-6, TNF-α CXCL10 (IP-10), CCL3 (MIP1-α) and CCL5 (RANTES) were significantly higher in 10^5PFU infected hamsters (Figure 6A). The expression of death receptor TRAIL and pro-apoptotic gene PUMA were significantly upregulated in 10^3PFU and 10^5PFU challenged hamsters, respectively (Figure 6B). This suggested that inflammatory cytokine responses were associated with testicular pathology. The abundancy of TUNEL staining signal varied, TUNEL positive cells were minimal in mock-control, while found in multiple seminiferous tubules after SARS-CoV-2 infection. The semiquantitative TUNEL positive scores increased with increasingly higher virus inoculum at 4dpi (Figure 6C&D).

Histopathological changes of chronic testicular damage after SARS-CoV-2 infection

At 42dpi and 120dpi after intranasal 10^3PFU challenge, various degree of seminiferous epithelial degeneration including disorganized germ cells, sloughed cells, seminiferous tubular necrosis filled with luminal cell debris, severe spermatogenic cell depletion and loss of spermatozoa persisted (Figure 7A-B). Johnsen's scores indicated severe impairment of spermatogenesis(Figure 3E). The percentages of hamsters showing testicular histopathological damages at 42dpi and 120dpi were 57.1%(4/7) and 71.4%(5/7), respectively (Table 1). The epididymal lumen of epididymis at 42 or 120dpi contained few or no sperm with just cell debris. Unexpectedly, mRNA levels of inflammatory cytokine/chemokine at 42 and 120dpi were similar to mock-control (Figure 7C). However, expression of death receptor genes TRAIL, and pro-apoptosis gene BAX were still elevated

at 120dpi, suggesting progressive pathology. TUNEL staining showed more extensive positive signals in seminiferous tubules at 120dpi than 42dpi (Figure 7D&E). Immunofluorescent staining by mouse anti-hamster IgG showed extensive staining on cell surfaces of necrotic seminiferous tubules at 7 to 120dpi, with patches of positive complement component 3 (C3), suggesting complement fixation by immune complex deposits at 7dpi (Figure 8 A-F). These findings further suggested that blood-testicular-barrier was breached [19, 20] and immune complex deposition might cause the testicular damages.

Testicular damages after intranasal challenge by multiple SARS-CoV-2 variant strains but not by A(H1N1)pdm09

To answer whether testicular damage is SARS-CoV-2 strain-specific, we intranasally challenged groups of 3 hamsters with 10^3PFU of Delta (B.1.617.2) and Omicron (B1.1.529) variants. At 4dpi, pneumonia occurred in all 6 hamsters with bronchiolitis, alveolitis and endotheliitis (Figure S3), while the severity was less in Omicron infected hamsters. Degeneration and necrosis of seminiferous tubules with various severities were observed in testes of Delta (2/3) or Omicron (2/3) infected hamsters at 4dpi and 7dpi(Figure 9A). Possibly due to more inflammatory edema at 4dpi, Omicron infected testes were significantly heavier than mock, but became significantly lighter than mock-control at 7dpi (Figure 9B). Sperm counts from Delta and Omicron infected hamsters were significantly reduced at 4 and 7dpi, respectively (Figure 9C).

Serum levels of testosterone, but not inhibin B was significantly reduced at 7dpi after Omicron or Delta infection (Figure 9D). Viral load was detected in some testes at 4dpi (Figure 9E). However, intranasal challenge with 10^3 or 10^5PFU of A(H1N1)pdm09 did not cause any histopathological changes in the testes at 4dpi (Figure 9F), despite finding interstitial pneumonia in infected hamsters (Figure S3).

Vaccination protected testicular damage after SARS-CoV-2 challenge

Hamsters immunized with two doses of intramuscular inactivated whole virion vaccine 14 days apart [14] were intranasally challenged with 10^3PFU of SARS-CoV-2 HK-13 14 days after second vaccination. Testes were examined at 4 and 28dpi (Figure 10A). Serum neutralizing antibodies were detected from all vaccinated animals after challenge at 4dpi and 28dpi, with GMT of 160±43.82 and 120±23.09, respectively. Testicles showed no histopathological changes in all nine vaccinated hamsters (Figure 10B). One group of hamsters (n=7) were challenged with 10^3PFU at 3 days after first vaccination showed no testicular histopathological damage at 4dpi (Figure 10B), indicating that vaccination effectively protects testes from SARS-CoV-2 infection.

DISCUSSION

Hamsters are now well established as a physiological small animal model for COVID-19 [12]. The animals recovered clinically by 28dpi. Here we showed that testicles were sub-clinically affected with acute decrease in sperm count and subsequent chronic asymmetric testicular atrophy associated with oligospermia and persistently low serum testosterone and inhibin B. These testes showed degeneration, necrosis and inflammation at both the interstitium with Leydig cells, and also seminiferous tubules with disruption of orderly spermatogenesis from 4 to 120dpi. Immunohistochemical staining of biomarkers showed that both Sertoli and germ cells of seminiferous tubules were severely affected. Viral N-protein expression was occasionally found in germ, interstitial and epididymal epithelial cells. These changes were generally more severe with higher virus inoculum. Moreover, intranasal challenge with wild-type SARS-CoV-2, Omicron or Delta variants could consistently cause testicular damage. To prove the causative role of SARS-CoV-2 in the pathogenesis of

testicular damage, we directly injected SARS-CoV-2 into the testicles transcutaneously which demonstrated far more positive N-protein expression in the interstitium and the presence of viral sgRNA in testicular tissue than with A(H1N1)pdm09 control virus.

Blood-borne and hepatitis viruses including HIV, HBV, HCV, and HEV are associated with subfertility and decreased sperm count or quality [21]. Clinical cases of coxsackie virus associated epididymo-orchitis are reported [22], but only mumps virus is convincingly associated with human orchitis [23, 24]. However, no animal models proving the causative role of these viruses in orchitis were reported. Filovirus with a prolonged high level of viremia [25], leading to severe haemorrhagic fever can lead to persistent infection of immunoprivileged organs including the central nervous system and the male reproductive tract in human and animal models [26]. Similarly, HEV infection can be associated with a prolonged viremia and subfertility in human [27]. Some arboviruses such as the Zika with prolonged viremia [28], is associated with sexual transmission, central nervous system infection, orchitis, and subfertility. Its causative role in epididymoorchitis is proven in an interferon α/β receptor deficient mice model. Here we showed that SARS-CoV-2, with absent or transient viremia could cause persistent testicular damage in the clinically relevant hamster model with self-limiting pneumonia.

Involvement of the male reproductive tract by SARS-CoV-2 has previously been suspected because angiotensin converting enzyme 2 (ACE2), the receptor for SARS-CoV-2, and/or transmembrane protease serine 2 (TMPRSS2), enzyme for proteolytic activation of spike, are abundantly expressed in spermatogonia, Sertoli, Leydig and myoid cells[29, 30]. Furthermore, case series of testicular or epididymal pain, histopathological changes of orchitis on postmortem examination, SARS-CoV-2 RNA detection in semen, reduced sperm

counts and serum testosterone level were also reported[31-34] . Besides conflicting clinical reports[8, 9], the testicular damage could be due to direct viral invasion or an indirect effect of systemic hypercytokinaemia, endotheliitis, vasculitis, thrombosis, and hypoxia due to respiratory failure or shock in severe COVID-19 [2]. Two previous hamster studies demonstrated very low viral load in testicles. However, one intranasal challenge study showed expression of testicular SARS-CoV-2 RNA without histopathological damages up to one month post-infection, despite the detection of viral replication in *ex vivo* hamster testicular cells[35]. Another hamster study only showed oophoritis but not orchitis despite patchy prostatitis and seminal vasculitis[36].

Here, we demonstrated that increasing infectious SARS-CoV-2 dose was associated with worsening testicular damage as evident by lower testicular weight at 120dpi and more severe and persistent histopathological changes. This may explain the high incidence of testicular changes found in deceased patients[33, 37]. The higher virus inoculum may increase the likelihood of SARS-CoV-2 crossing the blood-testicular-barrier into this immune-privileged organ. Though virus replication and leukocyte infiltration in testicles were far lower than lungs, we speculate that acute damage at 4 to 7dpi is more related to highly susceptible germ cells to the cytokine/chemokines produced by Sertoli cells and interstitial macrophages for innate immune response against the small amount of SARS-CoV-2 going across the blood-testicular-barrier[38]. While the testicular cytokine/chemokines normalized between 42 and 120dpi, the process of immune complex deposition and immunopathological damage might start after 7dpi. As expected, the tissue mRNA expression level of proinflammatory cytokine/chemokines with acute damage, and the apoptotic markers were associated with both acute and chronic testicular damage. This is consistent with the pathogenesis of mumps orchitis where mumps virus triggers type 1 interferons, TNF-a, IL-6, CXCL10, MCP1 which

induce apoptosis, disrupt blood-testicular- barrier, inhibit testosterone synthesis in Leydig cells and recruit inflammatory cells into testes[24].

To prove the causative role of SARS-CoV-2 in pathogenesis of testicular damage, we directly injected SARS-CoV-2 into animal testes to bypass the blood-testicular-barrier. More abundant N-protein expression was found in interstitial cells. Interstitial Leydig cells may be a target of SARS-CoV-2. Leydig cells are the primary source of testosterone in males. Its high concentration at seminiferous tubules is pivotal for maintaining testicular microvascular blood flow, Sertoli cell maturation, orderly spermatogenesis, and an intact blood-testicular-barrier. Intratesticular inoculation of mumps[39] and Zika[40] were used in rodent models of orchitis. Finally, we showed that vaccination given as late as 3 days before virus challenge could protect the animal testes against SARS-CoV-2 induced damage similar to the protection of their lungs[14]

Our findings here are limited to this hamster model. Few antibodies against hamster biomarkers for immunohistochemistry were available to locate infected cell types. We did not follow up beyond 120dpi due to limited availability of BSL3 facilities. In summary, SARS-CoV-2 can cause acute and chronic testicular damage in hamsters and is consistent with the anecdotal reports of clinical orchitis and hypogonadism in recovered COVID-19 males. Long term follow-up of sperm count and sex hormone profile of convalescent COVID-19 males is warranted.

Notes

Author contributions: *C.L., Z.H.Y.,* A. J. Z., J. F.-W. C., and K.-Y. Y. had roles in the study design, data collection, data analysis, data interpretation, and writing of the manuscript. W-C.S., F-F.L., Y-X.C., A.C-Y.L., Y.Z., B.H-Y. W., C.C-Y.Y., J-P.C. conducted part of the experiments. Y-W. K., D.L., S.S., D-Y.J., H.C. S.S. and K.K-W.T. had roles in the study design, experiments, data collection, and/or data analysis. All authors reviewed and approved the final version of the manuscript.

Ethical approval. The animal experiments in this study was approved by the HKU Committee on the Use of Live Animals in Teaching and Research (CULATR) and complied with the ARRIVE guidelines. Male Syrian hamsters were obtained from the Chinese University of Hong Kong Laboratory Animal Service Centre through the HKU Centre for Comparative Medicine Research.

Disclaimer. The funding sources had no role in the study design, data collection, analysis, interpretation, or writing of the report.

Financial support. This study was partly supported by funding from the Health and Medical Research Fund (COVID190121), the Food and Health Bureau, The Government of the Hong Kong Special Administrative Region; the Theme-Based Research Scheme (T11-709/21-N) of Research Grants Council, The Government of the Hong Kong Special Administrative Region; Health@InnoHK, Innovation and Technology Commission, the Government of the Hong Kong Special Administrative Region; the National Program on Key Research Project of China (2020YFA0707500 and 2020YFA0707504); National Natural Science Foundation of China Excellent Young Scientists Fund (Hong Kong and Macau) (32122001); Sanming Project of Medicine in Shenzhen, China (SZSM201911014); the High Level-Hospital Program, Health Commission of Guangdong Province, China; and the research project of Hainan Academician Innovation Platform (YSPTZX202004); the

Emergency Key Program of Guangzhou Laboratory (EKPG22-01); National Key Research and Development Programme on Public Security Risk Prevention and Control Emergency Project; the Consultancy Service for Enhancing Laboratory Surveillance of Emerging Infectious Diseases and Research Capability on Antimicrobial Resistance for Department of Health of the Hong Kong Special Administrative Region Government; the University of Hong Kong Outstanding Young Researcher Award; the University of Hong Kong Li Ka Shing Faculty of Medicine Research Output Prize; and donations of Michael Seak-Kan Tong, Richard Yu and Carol Yu, Shaw Foundation Hong Kong, May Tam Mak Mei Yin, the Providence Foundation (in memory of the late Lui Hac Minh), Lee Wan Keung Charity Foundation Limited, Hong Kong Sanatorium & Hospital, Respiratory Viral Research Foundation Limited, Hui Ming, Hui Hoy and Chow Sin Lan Charity Fund Limited, Chan Yin Chuen Memorial Charitable Foundation, Marina Man-Wai Lee, the Hong Kong Hainan Commercial Association South China Microbiology Research Fund, the Jessie & George Ho Charitable Foundation, Perfect Shape Medical Limited, Kai Chong Tong, Tse Kam Ming Laurence, Foo Oi Foundation Limited, Betty Hing-Chu Lee, Ping Cham So, and Lo Ying Shek Chi Wai Foundation.

Potential conflicts of interests. J.F.-W.C. has received travel grants from Pfizer Corporation Hong Kong and Astellas Pharma Hong Kong Corporation Limited and was an invited speaker for Gilead Sciences Hong Kong Limited and Luminex Corporation. K.K.-W.T. and K.-Y.Y. report collaboration with Sinovac Biotech Ltd. and China National Pharmaceutical Group Co., Ltd. (Sinopharm). The other authors declare no competing interests. All authors have submitted the ICMJE Form for Disclosure of Potential Conflicts of Interest.

REFERENCES

1. WHO. https://covid19.who.int/. **2022**.
2. To KK, Sridhar S, Chiu KH, et al. Lessons learned 1 year after SARS-CoV-2 emergence leading to COVID-19 pandemic. Emerg Microbes Infect **2021**; 10(1): 507-35.
3. Gupta A, Madhavan MV, Sehgal K, et al. Extrapulmonary manifestations of COVID-19. Nat Med **2020**; 26(7): 1017-32.
4. Ediz C, Tavukcu HH, Akan S, et al. Is there any association of COVID-19 with testicular pain and epididymo-orchitis? Int J Clin Pract **2021**; 75(3): e13753.
5. Xu J, Qi L, Chi X, et al. Orchitis: a complication of severe acute respiratory syndrome (SARS). Biol Reprod **2006**; 74(2): 410-6.
6. Killingley B, Mann A., Kalinova, M., . Safety, tolerability, and viral kinetics during SARS-CoV-2 human challenge. Nature Portfolio Journal **2022**.
7. Singh B, Gornet M, Sims H, Kisanga E, Knight Z, Segars J. Severe Acute Respiratory Syndrome Coronavirus 2 (SARS-CoV-2) and its effect on gametogenesis and early pregnancy. Am J Reprod Immunol **2020**; 84(5): e13351.
8. Li D, Jin M, Bao P, Zhao W, Zhang S. Clinical Characteristics and Results of Semen Tests Among Men With Coronavirus Disease 2019. JAMA Netw Open **2020**; 3(5): e208292.
9. Pan F, Xiao X, Guo J, et al. No evidence of severe acute respiratory syndrome-coronavirus 2 in semen of males recovering from coronavirus disease 2019. Fertil Steril **2020**; 113(6): 1135-9.
10. Chu H, Chan JF, Yuen TT, et al. Comparative tropism, replication kinetics, and cell damage profiling of SARS-CoV-2 and SARS-CoV with implications for clinical manifestations, transmissibility, and laboratory studies of COVID-19: an observational study. Lancet Microbe **2020**; 1(1): e14-e23.
11. Zhang AJ, Lee AC, Chan JF, et al. Coinfection by Severe Acute Respiratory Syndrome Coronavirus 2 and Influenza A(H1N1)pdm09 Virus Enhances the Severity of Pneumonia in Golden Syrian Hamsters. Clin Infect Dis **2021**; 72(12): e978-e92.
12. Chan JF, Zhang AJ, Yuan S, et al. Simulation of the Clinical and Pathological Manifestations of Coronavirus Disease 2019 (COVID-19) in a Golden Syrian Hamster Model: Implications for Disease Pathogenesis and Transmissibility. Clin Infect Dis **2020**; 71(9): 2428-46.
13. Chu H, Chan JF, Wang Y, et al. Comparative Replication and Immune Activation Profiles of SARS-CoV-2 and SARS-CoV in Human Lungs: An Ex Vivo Study With Implications for the Pathogenesis of COVID-19. Clin Infect Dis **2020**; 71(6): 1400-9.
14. Li C, Chen YX, Liu FF, et al. Absence of Vaccine-enhanced Disease With Unexpected Positive Protection Against severe acute respiratory syndrome coronavirus 2 (SARS-CoV-2) by Inactivated Vaccine Given Within 3 Days of Virus Challenge in Syrian Hamster Model. Clin Infect Dis **2021**; 73(3): e719-e34.
15. Zhang AJ, Lee AC, Chu H, et al. Severe Acute Respiratory Syndrome Coronavirus 2 Infects and Damages the Mature and Immature Olfactory Sensory Neurons of Hamsters. Clin Infect Dis **2021**; 73(2): e503-e12.
16. Li C, Chen Y, Zhao Y, et al. Intravenous injection of COVID-19 mRNA vaccine can induce acute myopericarditis in mouse model. Clin Infect Dis **2021**.
17. Teixeira TA, Pariz JR, Dutra RT, Saldiva PH, Costa E, Hallak J. Cut-off values of the Johnsen score and Copenhagen index as histopathological prognostic factors for postoperative semen quality in selected infertile patients undergoing microsurgical correction of bilateral subclinical varicocele. Transl Androl Urol **2019**; 8(4): 346-55.
18. Dang-Cong T N-TT. Male Reproductive Anatomy London London: IntechOpen, **2021**.
19. Umaoka A, Takeuchi H, Mizutani K, et al. Skin Inflammation and Testicular Function: Dermatitis Causes Male Infertility via Skin-Derived Cytokines. Biomedicines **2020**; 8(9).

20. Dulin JN, Moore ML, Gates KW, Queen JH, Grill RJ. Spinal cord injury causes sustained disruption of the blood-testis barrier in the rat. PLoS One **2011**; 6(1): e16456.
21. Garolla A, Pizzol D, Bertoldo A, Menegazzo M, Barzon L, Foresta C. Sperm viral infection and male infertility: focus on HBV, HCV, HIV, HPV, HSV, HCMV, and AAV. J Reprod Immunol **2013**; 100(1): 20-9.
22. Vuorinen T, Osterback R, Kuisma J, Ylipalosaari P. Epididymitis caused by coxsackievirus A6 in association with hand, foot, and mouth disease. J Clin Microbiol **2014**; 52(12): 4412-3.
23. Wu H, Wang F, Tang D, Han D. Mumps Orchitis: Clinical Aspects and Mechanisms. Front Immunol **2021**; 12: 582946.
24. Wu H, Shi L, Wang Q, et al. Mumps virus-induced innate immune responses in mouse Sertoli and Leydig cells. Sci Rep **2016**; 6: 19507.
25. Vetter P, Fischer WA, 2nd, Schibler M, Jacobs M, Bausch DG, Kaiser L. Ebola Virus Shedding and Transmission: Review of Current Evidence. J Infect Dis **2016**; 214(suppl 3): S177-S84.
26. Schindell BG, Webb AL, Kindrachuk J. Persistence and Sexual Transmission of Filoviruses. Viruses **2018**; 10(12).
27. Huang F, Long F, Yu W, et al. High prevalence of hepatitis E virus in semen of infertile male and causes testis damage. Gut **2018**; 67(6): 1199-201.
28. Mansuy JM, Mengelle C, Pasquier C, et al. Zika Virus Infection and Prolonged Viremia in Whole-Blood Specimens. Emerg Infect Dis **2017**; 23(5): 863-5.
29. Qi J, Zhou Y, Hua J, et al. The scRNA-seq Expression Profiling of the Receptor ACE2 and the Cellular Protease TMPRSS2 Reveals Human Organs Susceptible to SARS-CoV-2 Infection. Int J Environ Res Public Health **2021**; 18(1).
30. Wang Z, Xu X. scRNA-seq Profiling of Human Testes Reveals the Presence of the ACE2 Receptor, A Target for SARS-CoV-2 Infection in Spermatogonia, Leydig and Sertoli Cells. Cells **2020**; 9(4).
31. Gagliardi L, Bertacca C, Centenari C, et al. Orchiepididymitis in a Boy With COVID-19. Pediatr Infect Dis J **2020**; 39(8): e200-e2.
32. Ozveri H, Eren MT, Kirisoglu CE, Sariguzel N. Atypical presentation of SARS-CoV-2 infection in male genitalia. Urol Case Rep **2020**; 33: 101349.
33. Yang M, Chen S, Huang B, et al. Pathological Findings in the Testes of COVID-19 Patients: Clinical Implications. Eur Urol Focus **2020**; 6(5): 1124-9.
34. Flaifel A, Guzzetta M, Occidental M, et al. Testicular Changes Associated With Severe Acute Respiratory Syndrome Coronavirus 2 (SARS-CoV-2). Arch Pathol Lab Med **2021**; 145(1): 8-9.
35. Campos RK, Camargos VN, Azar SR, Haines CA, Eyzaguirre EJ, Rossi SL. SARS-CoV-2 Infects Hamster Testes. Microorganisms **2021**; 9(6).
36. Song Z, Bao L, Yu P, et al. SARS-CoV-2 Causes a Systemically Multiple Organs Damages and Dissemination in Hamsters. Front Microbiol **2020**; 11: 618891.
37. Ma X, Guan C, Chen R, et al. Pathological and molecular examinations of postmortem testis biopsies reveal SARS-CoV-2 infection in the testis and spermatogenesis damage in COVID-19 patients. Cell Mol Immunol **2021**; 18(2): 487-9.
38. Jiang Q, Wang F, Shi L, et al. C-X-C motif chemokine ligand 10 produced by mouse Sertoli cells in response to mumps virus infection induces male germ cell apoptosis. Cell Death Dis **2017**; 8(10): e3146.
39. Pickar A, Xu P, Elson A, et al. Establishing a small animal model for evaluating protective immunity against mumps virus. PLoS One **2017**; 12(3): e0174444.
40. Ma W, Li S, Ma S, et al. Zika Virus Causes Testis Damage and Leads to Male Infertility in Mice. Cell **2016**; 167(6): 1511-24 e10.

FIGURE LEGENDS

Figure 1. Intranasal inoculation of SARS-CoV-2 causes acute testicular damage in golden Syrian hamsters

A. Schema of intranasal challenge of male Syrian hamsters at 8-10 weeks of age. The animals were randomly divided into groups and intranasally challenged by SARS-CoV-2 HK-13 strain at a dose of 10, 10^2, 10^3 and 10^5 PFU in 50ul. The animals were monitored and sacrificed at 1, 4, 7, for study of acute damages, and at 42dpi or 120dpi for chronic damages.

B. Sperm counts. The epididymis was dissected and opened, sperms were rinsed out for counting the number per hamster testicle. n=5-10 for each group. Data represent mean ± SD. * $p<0.05$, ** $p<0.01$ by Student's t-test comparing to mock-controls.

C. Average weight of testis. After removing the epididymis, the testes were measured for wet weight immediately. n=5-10 for each group. Data represent mean ± SD.

D. Representative images of gross pathology of testes from SARS-CoV-2 infected group and mock-controls. The images showed no apparent changes of size and color at 1, 4 or 7dpi comparing to mock-control. Scale bar=1cm.

E. Serum concentration of sex hormones determined by ELISA. Serum samples were collected at 1, 4 or 7dpi after 10^3 or 10^5 PFU of SARS-CoV-2 HK-13 strain for assays of testosterone and inhibin B. n=5-13 for each group. Data represent mean ± SD. * $p<0.05$, ** $p<0.01$ by Student's t-test comparing to mock-controls.

Abbreviations: SARS-CoV-2, Severe Acute Respiratory Syndrome Coronavirus 2; dpi, days post infection; PFU, plaque forming unit.

Figure 2. Intranasal SARS-CoV-2 challenge causes chronic testicular damage in golden Syrian hamster. Male hamsters at 8-10 weeks of age were intranasally inoculated with 10^3 PFU of wild-type SARS-CoV-2 HK-13 stain in 50ul. The animals were monitored and scarified at 42 or 120dpi.

A. Representative images of gross pathology of testicles after SARS-CoV-2 infection and age-matched mock-controls. The images showed reduced size of testes at 120dpi, while no apparent changes at 42dpi compared to mock-controls. Scale bar=1cm.

B. Average weight of testes. After removing the epididymis, the testis was measured for wet weight immediately. n=5-7 for each group. Data represent mean ± SD. ** p<0.01 by Student's t-test comparing to mock-controls.

C. Sperm counts. The epididymis was dissected and the number of sperms was counted per hamster testicle. n=5-7 for each group. Data represent indicate mean ± SD. ** p<0.01, *** p<0.001 by Student's t-test comparing to mock-controls.

D. Serum concentration of testosterone and inhibin B determined by ELISA. n=4-7 for each group. Data represent mean ± SD. ** p<0.01 by Student's t-test comparing to mock-controls.

Abbreviations: SARS-CoV-2, Severe Acute Respiratory Syndrome Coronavirus 2; dpi, days post infection; PFU, plaque forming unit.

Figure 3. Histopathological changes in the testicle of Syrian hamster challenged intranasally with SARS-CoV-2 at 4 or 7dpi. SARS-CoV-2 HK-13 strain was intranasally inoculated at a dose of 10, 10^2, 10^3 and 10^5 PFU in 50µl per animal. Testicles were harvested at 4 or 7dpi and immediately fixed in neutral formalin. Paraffin sections were stained by Haematoxylin and Eosin (H&E) for microscopic examination.

A. Illustration (left) and representative images of H&E stained testicular section of mock-control showing neatly arranged testicular structure, seminiferous tubules and different cell

types including Sertoli cells and germ cells at various differentiation stages with spermatozoa in the lumen of seminiferous tubules. Scale bar=500μm, 100μm or 50μm.

B. Representative H&E images of testicular tissues of hamsters intranasally challenged with 10^5 PFU SARS-CoV-2 at 4dpi. Interstitial inflammatory damages included hemorrhage, exudation with cellular infiltrates, and seminiferous tubule luminal edema (*) were shown in the left two images. Extensive interstitial and seminiferous tubular immune cell infiltration were shown in the images on the right, boxed area was magnified for showing mononuclear cell infiltrates. Scale bar=100μm.

C. Representative H&E images of testicular tissues of hamsters intranasally challenged with 10^5 PFU SARS-CoV-2 at 4dpi showed diffusely distributed abnormal seminiferous tubules and enlarged lumen without spermatozoa (*); reduced germinal cell spectrum (layers) and disordered cellular arrangement in most seminiferous segments (solid arrows). Degeneration of germ cells forming multi-nucleated giant cells were indicated by thin arrows. Severe seminiferous tubular necrosis (**) with luminal cells debris and infiltrated polymorph-nucleated cells in the magnified boxed area, were indicative of neutrophil infiltration. Scale bar=100μm or 50μm.

D. Representative H&E images of testicular tissues of hamsters intranasally challenged with 10^5 PFU SARS-CoV-2 at 7dpi. The left two images showed inflammatory infiltration and edema in the interstitium and lumen of expanded seminiferous tubules (*). Severe diffuse seminiferous tubular epithelial necrosis with cell debris filled the lumen. Spermatogenic cells were loosened and sloughed (two images on the right). Scale bar=200μm, or 100μm.

E. Scores for the spermatogenic epithelium. The integrity of germinal epithelium in seminiferous tubules were semi-quantitatively assessed by Johnsen's score with minor modifications. Since the histological damages caused by SARS-CoV-2 infection are patchily distributed in most of the testicular sections, 10 microscopic fields at 200x magnification

across the damaged area were randomly sampled with 35 tubules for each sample. Seminiferous germinal maturation was scored from 1 to 10, a score of 10 indicates full epithelial maturation, while a score of 1 means no germinal epithelium in the seminiferous tubules. The final Johnsen's score for a given sample was calculated by the sum of each seminiferous tubule score divided by 35. n=6-8. Data represent mean ± SD. ** p<0.01 by Student's t-test comparing to mock-controls.

F. Representative H&E images of epididymis of mock or 10^5 PFU SARS-CoV-2 challenged hamsters at 4dpi and 7dpi. The epididymal lumens of mock-control were filled with mature sperm, while those of infected hamsters contained large amount of sloughed germ cells and cell debris with much reduced sperms. Interstitial mononuclear immune cells infiltration was found in tissues at both 4dpi and 7dpi. Scale bar=200μm, or 100μm.

Abbreviations: SARS-CoV-2, Severe Acute Respiratory Syndrome Coronavirus 2; dpi, days post infection; PFU, plaque forming unit. H&E, Hematoxylin and Eosin.

Figure 4. Immunohistochemical staining of Sertoli cells and spermatogenic cells in testicular tissue of Syrian hamster challenged by SARS-CoV-2 at 4dpi.

A. Representative images of Sertoli cell biomarker vimentin in testis of mock-control. The images showed normal seminiferous tubules (left), the Sertoli cells with cytoplasmic vimentin regularly distributed in radiant pattern from the basal membrane, their cytoplasmic arms extend toward the lumen (open arrows). Scale bar=100 μm or 50μm.

B. Representative images of testes tissue of hamsters intranasally challenged by 10^5 PFU SARS-CoV-2 at 4dpi. Vimentin expressing Sertoli cells were deformed and detached from basal membrane (left, and magnified squared area); The images on the right showed Sertoli cells cytoplasmic vacuolation degeneration and loss of cytoplasmic arms (open arrows in magnified squared area). Scale bar= 50μm.

C. Representative images of Deleted In Azoospermia Like (DAZL) protein in testicular section of mock-control. The low magnification images showed that DAZL was highly expressed and evenly distributed in seminiferous tubular epithelium; higher power image in the middle and magnified squared area showed extensive and high level expression of DAZL in primary spermatocytes (solid arrows) and reduced level in spermatogonia (arrowheads), while the secondary spermatocytes were negative (thin arrows). Open arrows indicated Sertoli cells which were negative for DAZL. Scale bar=100 μm or 50μm.

D. Representative images of DAZL expression in testes of hamsters intranasally challenged by 10^5 PFU SARS-CoV-2 at 4dpi. The left two images showed DAZL expressing germinal cells were disarranged, detached or in form of multinucleated giant spermatocyte (solid arrows), spermatogonia was absent from the two severely damaged seminiferous tubules (area in dashed line), the thin arrows indicate multi-nucleated giant cells which is DAZL negative suggestive of degenerated secondary spermatocytes. The image on the right and magnified showed the sloughed germ cells were both DAZL positive and negative. Scale bar=100 μm or 50μm.

E. Images of H&E stained testicular tissues showing the morphology of interstitial Leydig cells. The Leydig cells were found in the interstitial space of mock-control testicular section (left image and magnified squared area, open arrowheads). Testis of hamster intranasally challenged by SARS-CoV-2 at 4dpi showed two Leydig cells with condensed nuclei indicative of apoptosis (right image and magnified squared area, open arrowheads). Scale bar=100μm or 50μm.

Abbreviations: SARS-CoV-2, Severe Acute Respiratory Syndrome Coronavirus 2; dpi, days post infection; PFU, plaque forming unit. H&E, Hematoxylin and Eosin; DAZL, Deleted In Azoospermia Like protein.

Figure 5. Viral load and viral antigen expression in testicles after intranasal or intratesticular inoculation of SARS-CoV-2.

A. Viral load in homogenized testicular tissue and lungs were determined by qRT-PCR. Data presented as copies of RdRp gene per copy of β-actin in log scale. Data represent indicate mean ± SD. n=5-15 for each group. Horizontal dashed line indicates the cut off for testicular viral load.

B. Representative images of immunofluorescence stained viral N protein in testes (upper panel) and epididymis (lower panel) of hamsters at 4dpi post intranasal challenged by 10^3 PFU of SARS-CoV-2. SARS-CoV-2 N protein (green) positive cells indicated by arrows in original and magnified images. Scale bar=100μm or 50μm.

C. Representative images of immunofluorescent viral N protein in sperm sample smear slides prepared from hamsters intranasally challenged by10^3 PFU SARS-CoV-2 at 4 dpi. SARS-CoV-2 N protein (green) positive cells (a sloughed cell) indicated by arrows in original and magnified images; scale bars=50μm.

D. Representative H&E images and immunofluorescent viral N protein in the testes of hamsters at 1 or 4 days after intratesticular injection (dpi)of 10^5 PFU of SARS-CoV-2 in 50μl under anesthesia. The H&E images showed interstitial congestion at 1dpi and mild seminiferous tubular degeneration and interstitial immune cells infiltration at 4dpi (thin arrows). Immunofluorescence stained SARS-CoV-2 viral N protein expressing cells were found in the interstitium of the testes at 1 and 4dpi after injection (arrows), SARS-CoV-2 viral N also found in the seminiferous epithelium which suggestive of germ cells. Representative N expressing cells were magnified in the inserts. Scale bar=200μm, 100μm or 50μm.

E. Representative images of immunofluorescent stained viral N protein in epididymis at 1 day after intratesticular injection. The images on the left showed N expressing epithelial cells

of epididymis (arrows in magnified image). The images on the right showed N positive spermatocytes in the lumen of epididymis Scale bar=50μm.

F. Viral load in the testes determined by qRT-PCR at 1 or 4 days after intratesticular injection of SARS-CoV-2. n=4-6 for each group. Data represent indicate mean±SD.

G. Determination of mRNA expression of inflammatory cytokine/chemokine by qRT-PCR in the homogenized testes at 1 or 4 days after injection of SARS-CoV-2 or same dose of influenza A(H1N)pdm09 virus (10^5 PFU) which was injected to another group of hamsters as controls. n=3-6 for each group. Data represent mean ± SD. * p<0.05, ** p<0.01, *** p<0.001, **** p<0.0001, by Student's t-test comparing to mock controls.

Abbreviations: SARS-CoV-2, Severe Acute Respiratory Syndrome Coronavirus 2; dpi, days post infection; PFU, plaque forming unit; RdRp, SARS-CoV-2 RNA-dependent-RNA-polymerase. DAPI, 4′ ,6-diamidino-2-phenylindole.

Figure 6. mRNA expression of inflammatory cytokine/chemokine and apoptosis regulatory genes and TUENL staining of testicular tissues from SARS-CoV-2 infected hamsters or mock-control animals. Testes collected at 4dpi after intranasal challenge by 10^3 or 10^5 PFU of SARS-CoV-2 were homogenized for total RNA extraction and qRT-PCR. The testes of infected animals showing various degree of histopathological damages comparing to mock-controls were included in this assay to compare cytokine/chemokine gene expression with mock controls.

A. Inflammatory cytokine and chemokine mRNA expression level in homogenized testes were determined by qRT-PCR with each gene specific primer. House-keeping gene β-actin was included for normalization of RNA concentration in each sample. The levels of relative gene expression were calculated by the ΔΔCt method relative to the mock-controls. n=7-9 for each group. Data represent mean ± SD. * p<0.05, ** p<0.01 by Student's t-test.

B. Apoptosis regulatory gene expression levels in homogenized testes at 4dpi after different doses of SARS-CoV-2 challenge. The relative mRNA expression was determined by qRT-PCR calculated by the ΔΔCt method. n=7-10 for each group. Data represent mean ± SD. * p<0.05, ** p<0.01 by Student's t-test**.**

C. Representative images of apoptosis marker TUNEL labeled testicular sections from 10^3 or 10^5 PFU SARS-CoV-2 infected hamster at 4dpi or mock control. One or two TUNEL positive cells were seen in mock-controls. Small foci of TUNEL positive cells in one seminiferous tubule after infection by 10^3 PFU SARS-CoV-2. Many TUNEL positive cells were shown in multiple seminiferous tubules after 10^5 PFU infection. Scale bar=200μm.

D. Semiquantitative scores for percentage TUNEL positive seminiferous tubules. The testes sections were labelled by Click-iT® Plus TUNEL assay kit and examined under fluorescent microscope. The TUNEL positive number of seminiferous tubules were semi-quantified from four random 100x magnification fields. Score 0, TUNEL positive seminiferous tubules <5% of total seminiferous tubules examined; score 1, 5–25%; score 2, 25–50%; score 3, 50–75%; and score 4, >75%. n=3-7 for each group. Data represent mean ± SD. * p<0.05, **** p<0.0001 by Student's t-test**.**

Abbreviations: SARS-CoV-2, Severe Acute Respiratory Syndrome Coronavirus 2; dpi, days post infection; PFU, plaque forming unit; IFN-α, interferon-α; IFN-γ, interferon-γ; TNF-α, tumor necrosis factor-α; IL-6, interleukine-6; IL-1β, interleukine-1β, CXCL10, C-X-C motif chemokine ligand 10 (or IP-10); CCL5, C-C Motif Chemokine Ligand 5 (or RANTES); CCL3, C-C Motif Chemokine Ligand 3(or MIP-1α), TRAIL, TNF-related apoptosis-inducing ligand; DR6, Death receptor 6; FasR, Fas receptor;TNFRSF1A, tumor necrosis factor receptor 1A ; BCL2, B-cell lymphoma 2; BAD, BCL2 associated agonist of cell death; PUMA, p53 upregulated modulator of apoptosis; NOXA, Phorbol-12-myristate-13-acetate-

induced protein 1; TUNEL, Terminal deoxynucleotidyl transferase dUTP nick end labeling. DAPI, 4′ ,6-diamidino-2-phenylindole.

Figure 7. Chronic testicular damages in 10^3 PFU SARS-CoV-2 infected hamsters at 42dpi or 120dpi and immunofluorescence staining of hamster IgG and complement C3 in testicular tissues.

A. Representative images of H&E stained tissue sections of testes and epididymis at 42dpi. The testes showed severe diffuse seminiferous tubular epithelial necrosis; spermatogenic cells were depleted in enlarged tubular lumen which contained little number of spermatozoa. The epididymal lumen contained large amount cell debris. Scale bar=200μm or 100μm.

B. Representative images of H&E stained testes at 120dpi. The germinal epithelium of seminiferous tubules showed atrophy and loss of normal differentiation spectrum. The epididymal lumen showed no sperm. Scale bar=200μm or 100μm.

C. mRNA expression of cytokine/chemokine and apoptosis regulating gene at 42 and 120dpi compared with those at the acute stage of 4 and 7dpi after same infective doses of 10^3 PFU of SARS-CoV-2. n=6-8 for each group. Data represent mean ± SD. Red curves indicate the mean expression level at each time point after infection.

D. Representative images of TUNEL stained testicular sections. The mock-control testis showed only one TUNEL positive cells, while significantly more abundant TUNEL positive cells were shown in the sections taken at 42 and 120dpi. Scale bar=200μm.

E. Scored for the intensity of TUNEL positive cells. The testes tissue sections were labelled by Click-iT® Plus TUNEL assay kit and examined under fluorescent microscope. The TUNEL positive seminiferous tubules were semi-quantified from four random 100x magnification fields. Score 0, TUNEL positive seminiferous tubules <5% of total seminiferous tubules examined; score 1, 5–25%; score 2, 25–50%; score 3, 50–75%; and

score 4, >75%. n=3-7 for each group. Data represent mean ± SD. **** p<0.0001 by Student's t-test.

Figure 8. Immunofluorescence stained hamster IgG and complement C3 in testicular tissues. Paraffin embedded testes samples collected at 1, 4, 7, 42 and 120dpi after 10^3 or 10^5 PFU SARS-CoV-2 intranasal inoculation were stained for the hamster IgG or C3 using goat anti-hamster IgG or C3 antibodies, respectively.

A. Representative images of immunofluorescence stain of hamster IgG in testicular tissues of mock-control. IgG staining signal was found only in the interstitium (thin arrows). No seminiferous tubular epithelial cells were positively stained. The dashed line circled area was magnified showing germ cells were negative of IgG. Scale bar=200μm or 100μm.

B. Representative images of IgG in testes of 1 and 4dpi after challenged with 10^5 PFU of SARS-CoV-2 intranasally. The IgG staining signals were found in interstitium. In the testes of 4dpi, the interstitial IgG was more intensely stained and seminiferous tubules in the dashed circle showed germ cell sloughing but no IgG labelled germ cells (solid arrows in magnified image). Scale bar=200μm or 100μm.

C. Representative images of IgG in testes of 7dpi after SARS-CoV-2 intranasal challenge. IgG staining signal in the interstitium (thin arrows), and extensive IgG signal was found inside seminiferous tubules where the germ cells were largely depleted (open arrows). In the seminiferous tubules with epithelium destruction (circled areas), IgG labelled the surface of germ cells which were disarranged or sloughed in the lumen of seminiferous tubules (solid arrows). Scale bar=200μm or 100μm.

D-E. Representative images of IgG in the testes of hamster at 42dpi (D) or 120dpi (E) after challenged by SARS-CoV-2 intranasally. The IgG staining intensity is reduced comparing to 7dpi. IgG mostly located in interstitium (thin arrows). Occasionally, IgG was found

precipitated in the seminiferous tubules and on the surface of sloughing germ cells (solid arrows in magnified circled area). Scale bar=200μm or 100μm.

F. Colocalization of complement C3 with IgG in hamster testicular tissues at 7dpi after challenged by SARS-CoV-2 intranasally. Complement C3 was occasionally found on the surface of germ cells in the same seminiferous tubule (circle areas) where IgG labelled germ cells were located. Scale bar=200μm or 100μm.

Abbreviations: SARS-CoV-2, Severe Acute Respiratory Syndrome Coronavirus 2; dpi, days post infection; PFU, plaque forming unit; IFN-α, interferon-α; IFN-γ, interferon-γ; TNF-α, tumor necrosis factor-α; IL-6, interleukine-6; IL-1β, interleukine-1β, CXCL10, C-X-C motif chemokine ligand 10 (or IP-10); CCL5, C-C Motif Chemokine Ligand 5 (or RANTES); CCL3, C-C Motif Chemokine Ligand 3(or MIP-1α), TRAIL, TNF-related apoptosis-inducing ligand; DR6, Death receptor 6; FasR, Fas receptor; TNFRSF1A, tumor necrosis factor receptor 1A ; BCL2, B-cell lymphoma 2; BAD, BCL2 associated agonist of cell death; PUMA, p53 upregulated modulator of apoptosis; NOXA, Phorbol-12-myristate-13-acetate-induced protein 1; TUNEL, Terminal deoxynucleotidyl transferase dUTP nick end labeling; C3, complement component 3. 4′,6-diamidino-2-phenylindole.

Figure 9. Multiple SARS-CoV-2 variant strains but not (H1N1)pdm09 influenza virus can cause testicular damage in hamsters. 10^3 PFU of each SARS-CoV-2 variant strains, including Delta (B.1.617.2) and Omicron (B.1.1.529) were intranasally inoculated into 6 hamsters per variant. Influenza A pdm(H1N1)2009 virus infection was performed as control. The animals were scarified at 4dpi and 7dpi. Lung, testicles and blood were taken for analysis.

A. Representative H&E images of testes at 4dpi and 7dpi after intranasal inoculation 10^3 PFU of Delta (B.1.617.2) or Omicron (B.1.1.529) variants. Various degrees of seminiferous tubular degeneration were shown. Scale bar=200μm.

B. Testes weight at 4dpi and 7dpi after Omicron or Delta virus challenge. n=3 for each infection group, n=7 for mock-control. Data represent mean ± SD. * p<0.05 by Student's t-test.

C. Sperm counts at 4dpi and 7dpi after Omicron or Delta virus challenge. n=3 for each infection group, n=7 for mock-control. Data represent mean ± SD. * p<0.05, ** p<0.01 by Student's t-test.

D. Serum concentration of testosterone and inhibin B in hamsters challenged by Delta or Omicron at 4dpi or 7dpi. n=3 for each infection group, n=4 for mock-control. Data represent mean ± SD. * p<0.05 by Student's t-test**.**

E. Viral load in homogenized testicular tissue at 4dpi and 7dpi were determined by qRT-PCR. Data presented as copies of RdRp gene per copy of β-actin in log scale. n=3 for each group. Data represent mean ± SD.

F. Representative H&E images of the testes and epididymis taken from hamsters intranasally infected by 10^3 or 10^5 PFU of (H1N1)pdm09 influenza virus. No histopathological changes were observed in testes or epididymis. Scale bar=500μm, 200μm or 100μm.

Abbreviations: SARS-CoV-2, Severe Acute Respiratory Syndrome Coronavirus 2; dpi, days post infection; PFU, plaque forming unit

Figure 10. Inactivated SARS-CoV-2 vaccine can protect hamsters from testicular damages despite intranasal challenged by SARS-CoV-2.

A. Schema of experimental procedure. Groups of hamsters were immunized with a two-dose vaccination via intramuscular injection of inactivated SARS-CoV-2 whole virion vaccine at 14 days apart. The animals were intranasally challenged by 10^3 PFU of SARS-CoV-2 at 14

days after second dose of vaccination, or at 3 days after the first dose of vaccination, testicles were examined at 4 and 28 days after SARS-CoV-2 challenge. Hamster received PBS injection as unvaccinated controls.

B. Summary of serum neutralizing antibody geometric mean titer (GMT) and representative H&E images of testes and epididymis at 4dpi and 28dpi after SARS-CoV-2 challenge. Scale bar=200μm.

Table 1. Summary of SARS-CoV-2 (10^3 PFU) causing testicular damages in Syrian hamsters

		Days post infection (dpi)			
		Acute damages		Chronic damages	
	Mock	4dpi	7dpi	42dpi	120dpi
Number of hamsters	14	17	6	7	7
Average Testes weight (g)	2.06±0.14	1.81±0.38	1.9±0.27	1.87±0.42	1.39±0.30**
Average sperm number ($\times 10^7$ cells/one side)	14.71±5.00	8.02±4.17**	7.81±5.78*	5.85±3.97**	2.50±3.27****
No. of hamster with testicular damage (%)	1/14 (7.14%)	8/17 (47.06%)†	4/6 (66.67%)†	4/7 (57.14%)†	5/7 (71.43%)††
Jonhsen's score for seminiferous tubule damage	8.87±1.53 (n=6)	6.16±1.39 (n=8)**	4.51±2.25**	6.44±0.51**	5.39±1.60**
TUNEL score for apoptosis	1±0 (n=8)	2.6±0.55 (n=5)****	2.67±1.15 (n=3)**	2.67±0.58 (n=3)****	2.8±0.84 (n=5)****
Serum Testosterone (ng/L)	822.97±87.39	591.69±251.91*	473.04±388.82	762.3±23.19	399.17±387.67*
Serum Inhibin-B (pg/mL)	194.83±61.99	114.55±77.35*	90.33±59.58*	69.75±79.33**	66.69±53.31**

*, $p<0.05$; **, $p<0.01$; ****, $p<0.0001$ comparing with mock by Student's t-test.

†, $p<0.05$; ††, $p<0.01$ comparing with mock by Fisher's exact test.

Figure 1

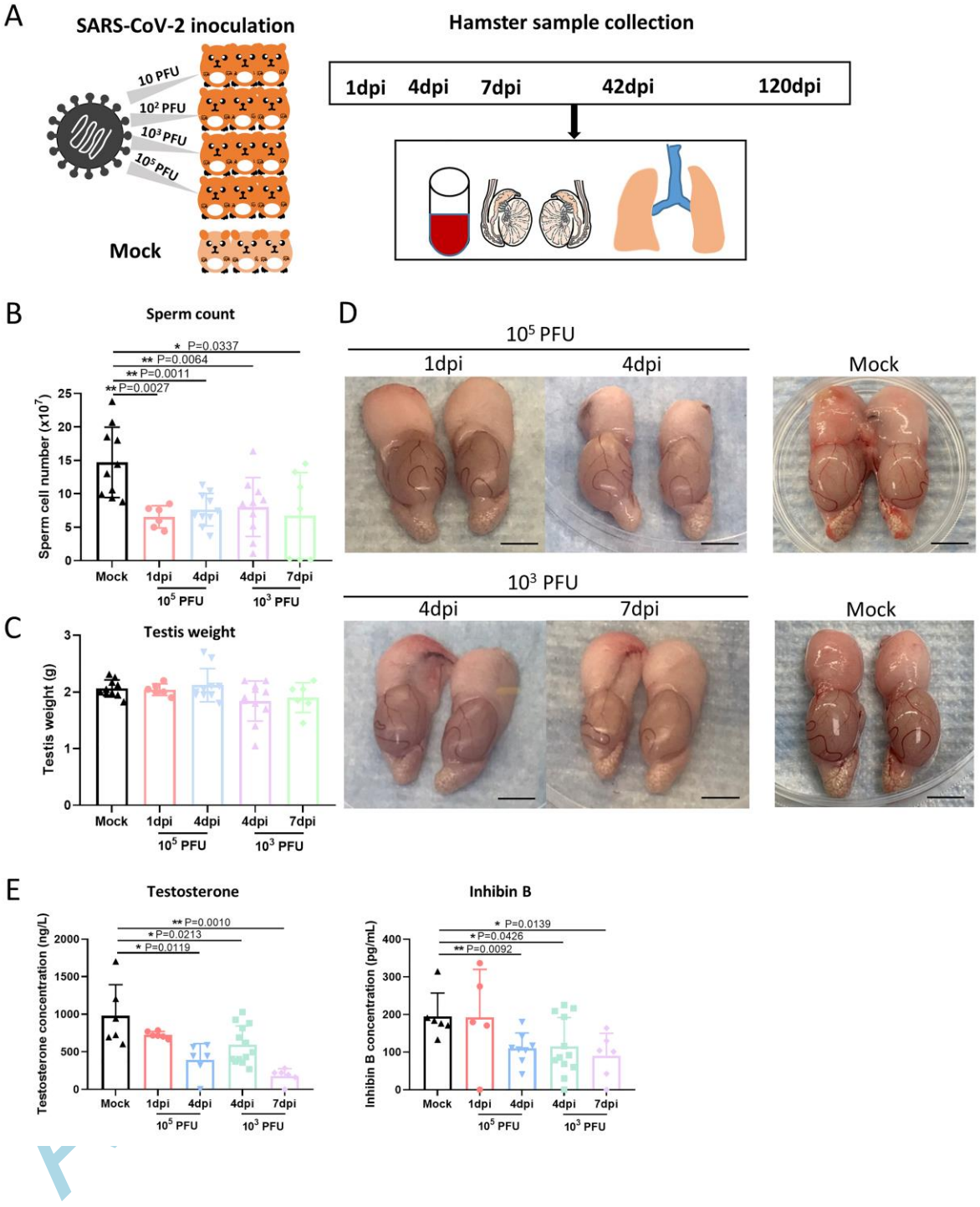

Figure 2

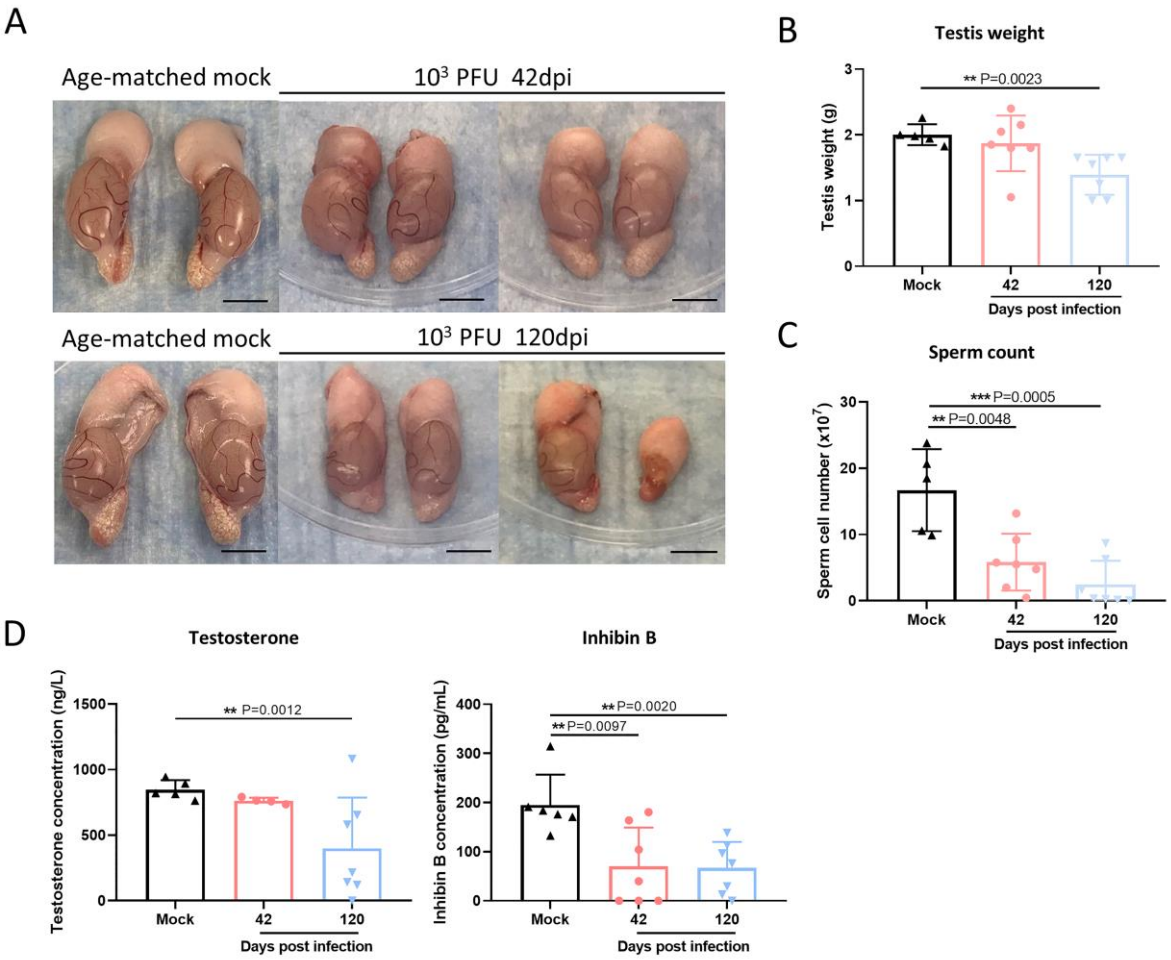

Figure 3

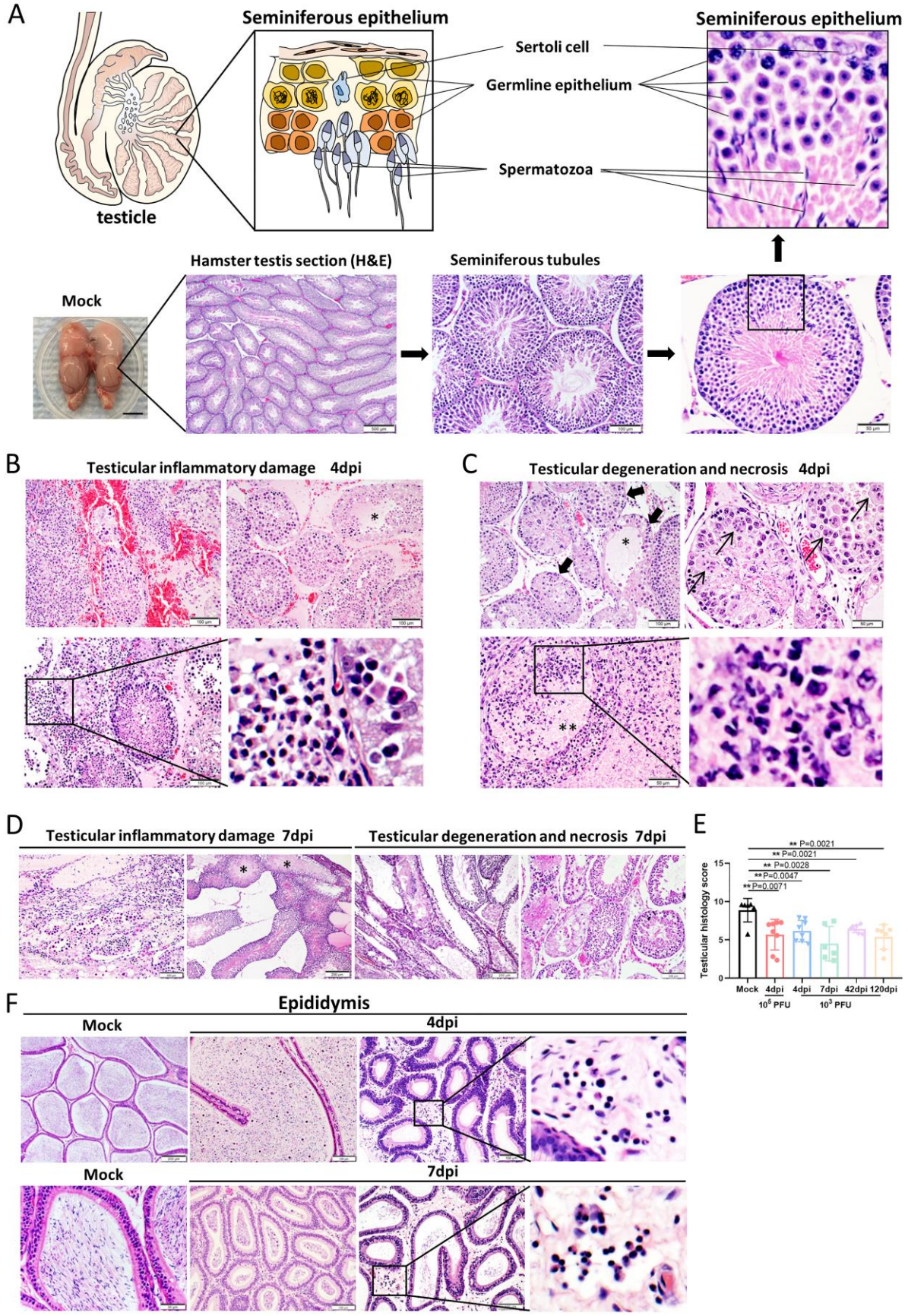

Figure 4

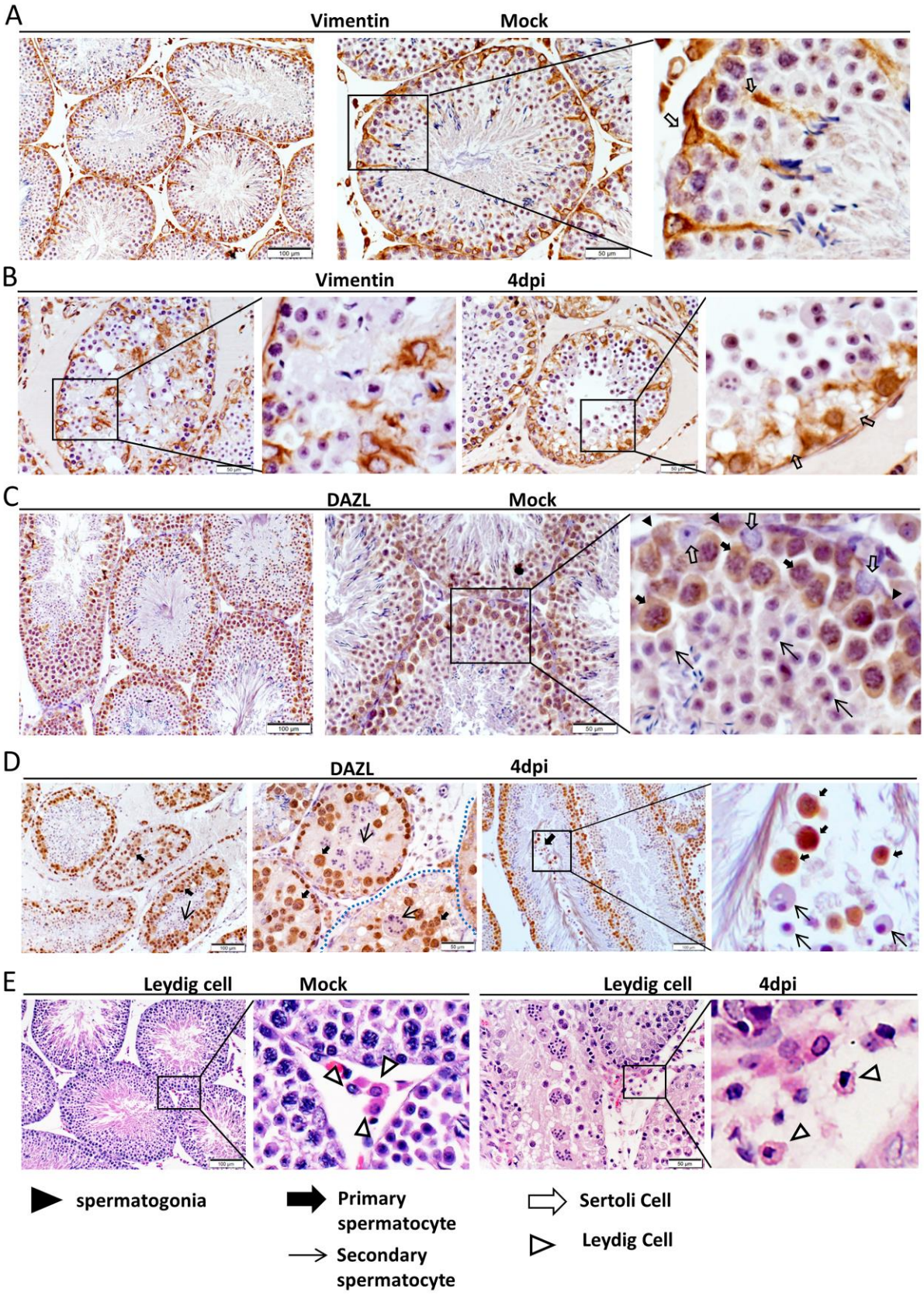

Figure 5

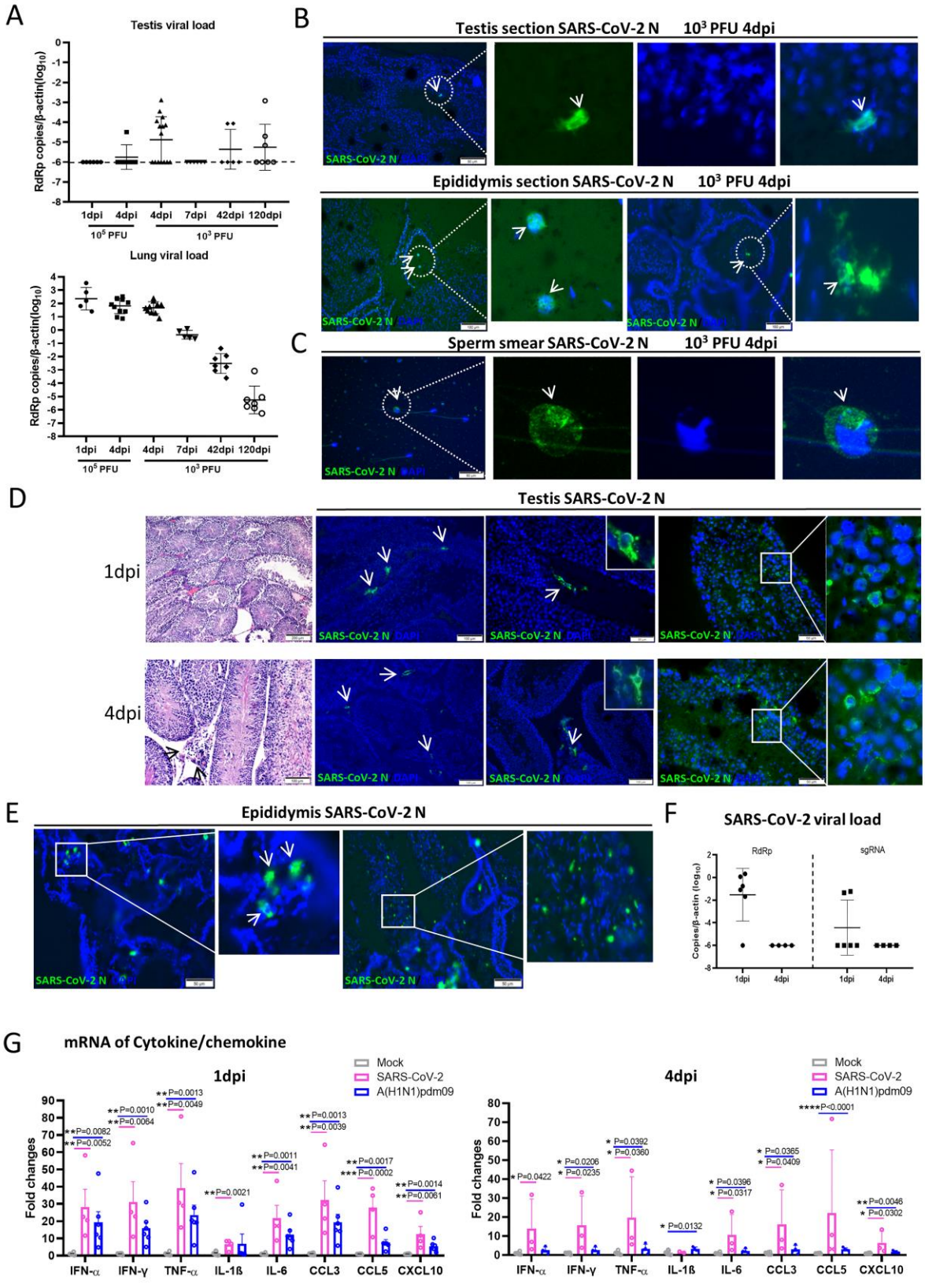

Figure 6

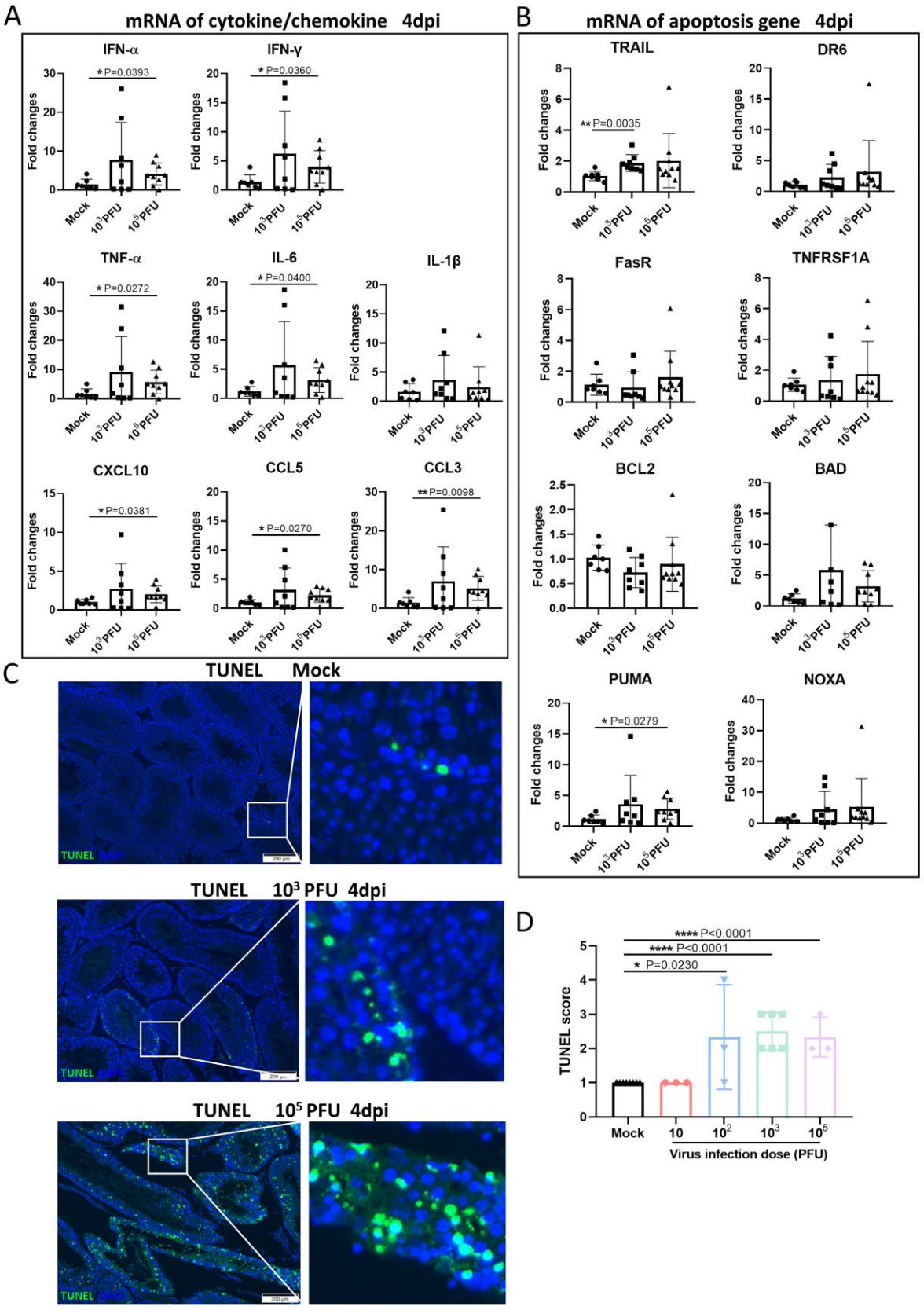

Figure 7

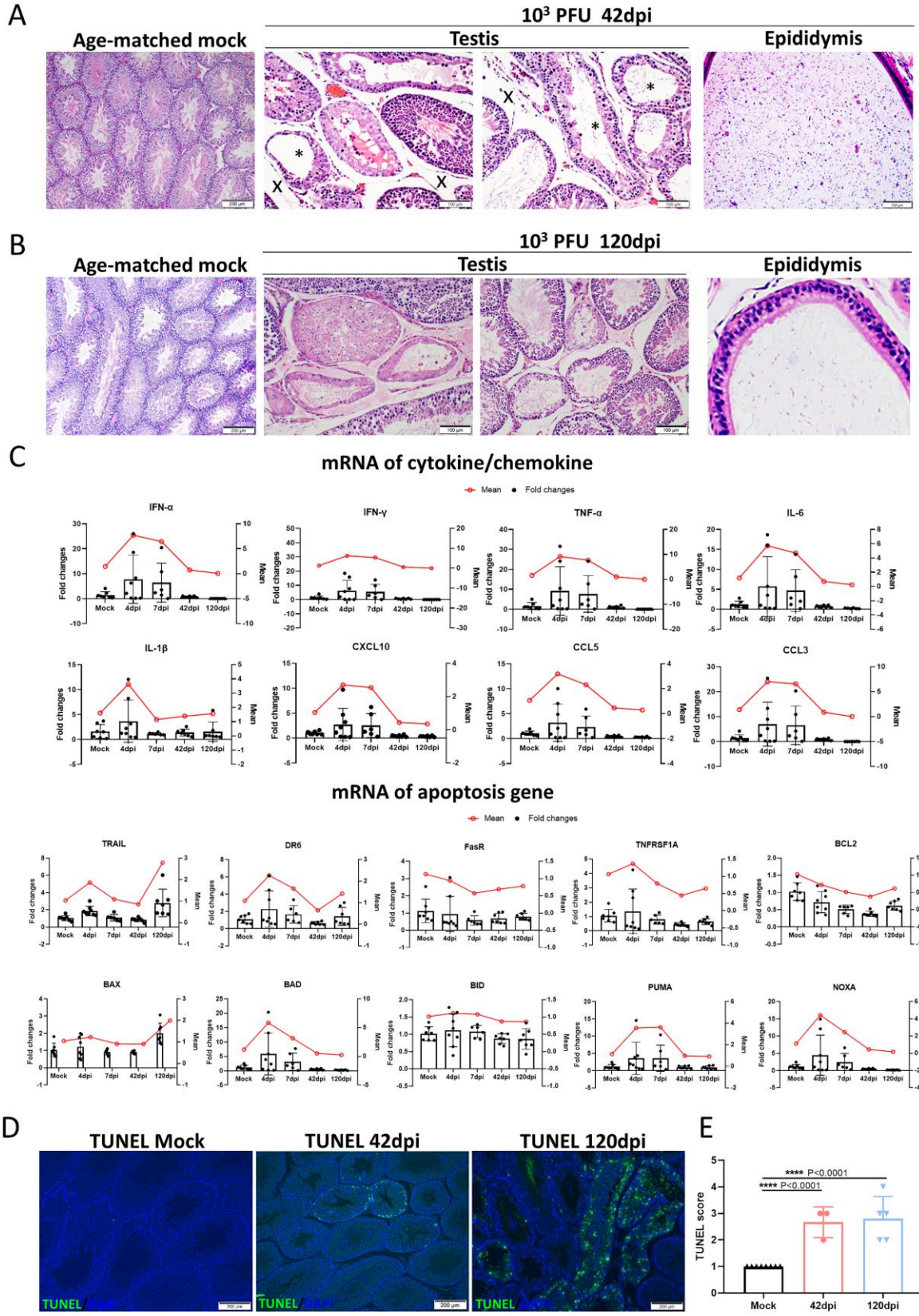

Figure 8

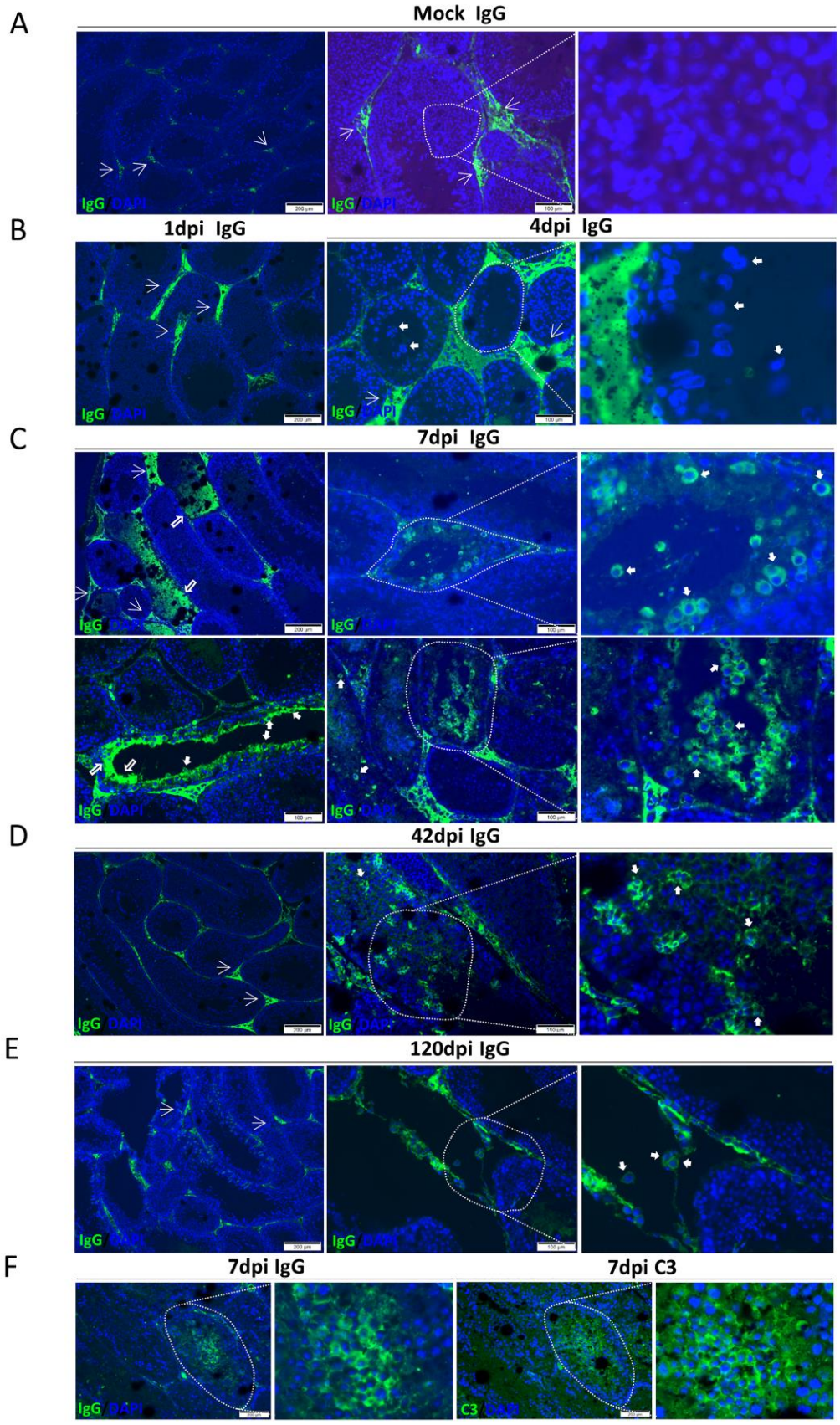

Figure 9

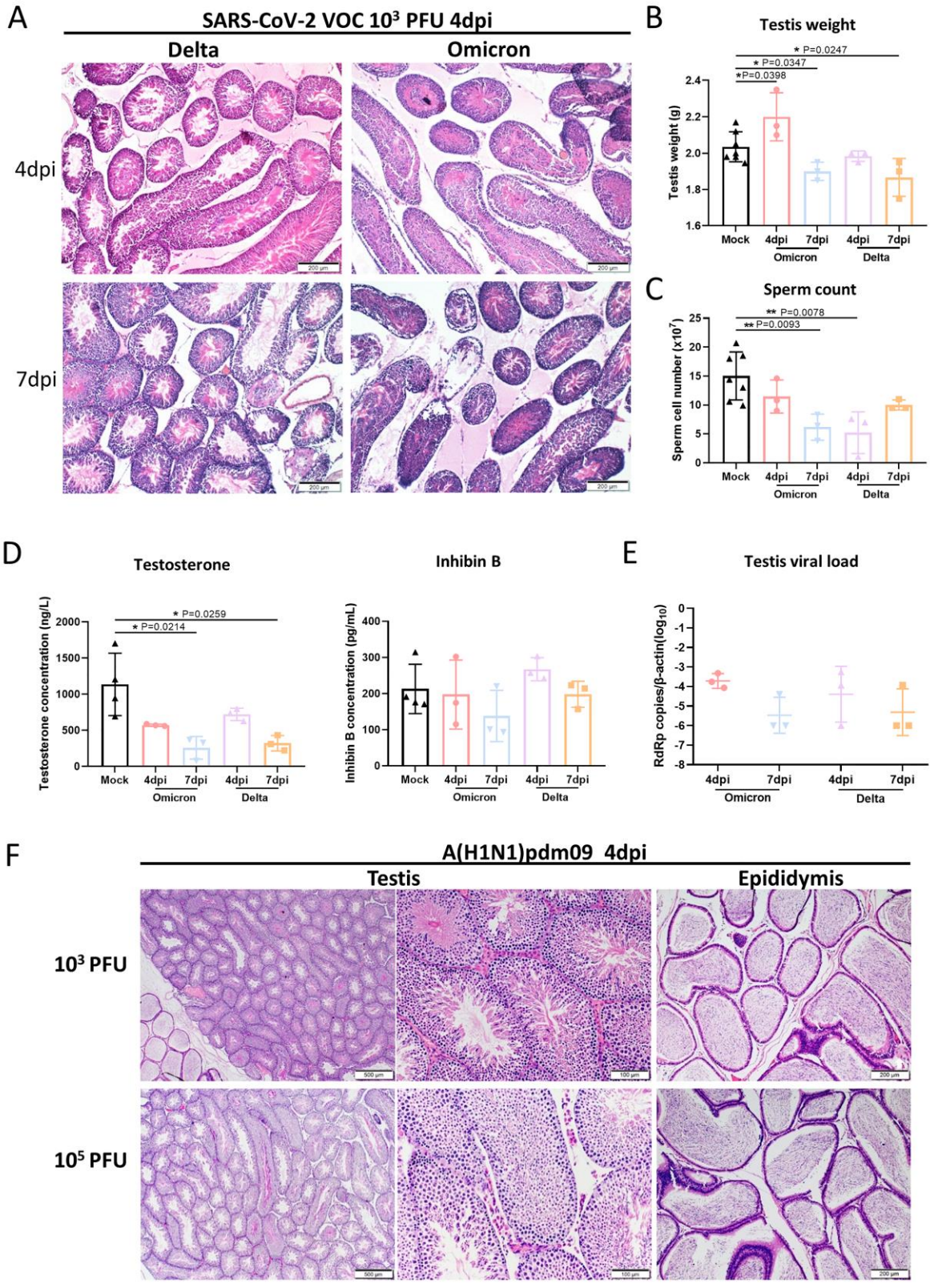

Figure 10

A

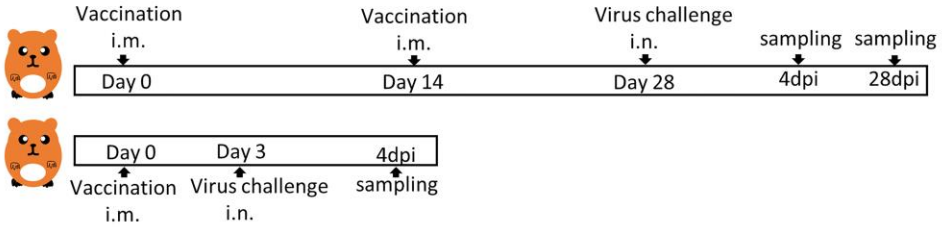

B

10^3 PFU of SARS-CoV-2 infection of vaccinated hamsters

	Days post infection	4dpi	28dpi	PBS 4dpi
Virus challenge 14 days after 2nd vaccination	Number of hamster	n=5	n=4	n=3
	Neutralizing Ab (GMT)	160.00±43.82	120.00±23.09	0.00±0.00
	Testicular damages	0/5	0/4	2/3
	Testis H&E	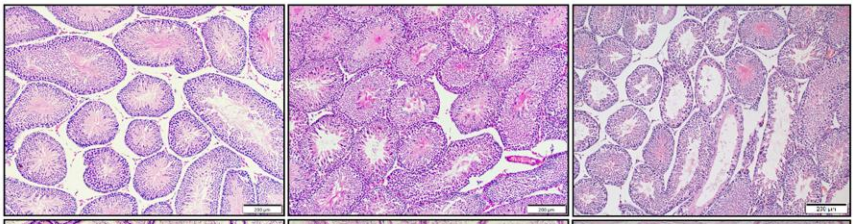		
	Epididymis H&E	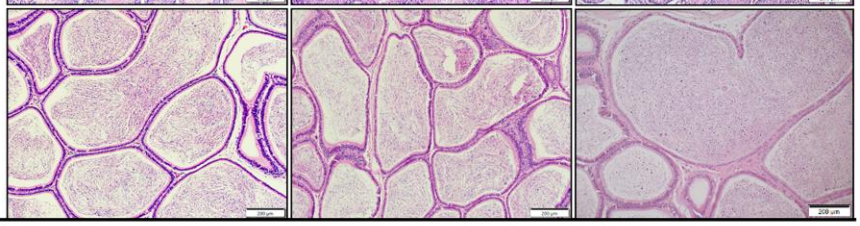		
Virus challenge 3 days after 1st dose vaccination	Number of hamster (n=7)	7	ND	
	Neutralizing Ab (GMT at 4dpi)	66.25±21.79	ND	
	Testicular damages	0/7	ND	
	Testis H&E	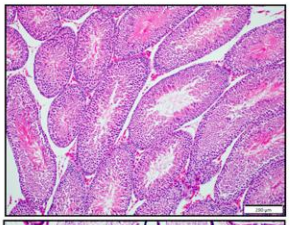	ND	
	Epididymis H&E	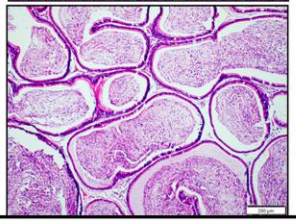	ND	